

Pressure dependence of the Mössbauer isomer shift for metallic Sb and for I^- in KI. Systematics with atomic number of the pressure dependence of $|\psi(0)|^2$

William T. Krakow,*† William D. Josephson,† P. A. Deane, D. L. Williamson,‡ and Louis D. Roberts

Department of Physics and Astronomy, University of North Carolina, Chapel Hill, North Carolina 27514

(Received 18 June 1980)

We have measured the pressure dependence of the Mössbauer isomer shift for metallic Sb and for I^- in KI. This pressure dependence is related to $\gamma = d|\psi(0)|^2/d\ln V$ and we have obtained values for $\gamma(\text{Sb})$ and $\gamma(I^-)$ from the Mössbauer results. For Sb, we find $\gamma(\text{Sb}) > 0$, viz., that $|\psi(0)|^2$ decreases when an antimony sample is compressed. For I^- in KI we find γ to have a value of zero within experimental error. The systematics of γ with atomic number are discussed.

I. INTRODUCTION

From high-pressure measurements of the Mössbauer isomer shift S it has been found that for pure metallic Fe¹, Ta², and Au³, the total electron charge density in contact with the nucleus, $|\psi(0)|^2$, increases when the sample is compressed.¹⁻⁴

Here the derivative $\gamma = d|\psi(0)|^2/d\ln V < 0$, where V is the atomic volume. This result may be expected if the compression of the atom should result, at least qualitatively, in a renormalization of the inner-atom valence-electron wave function.

In contrast to the above measurements of γ for Fe, Ta, and Au, Panyushkin and Voronov,⁵ and Möller and Mössbauer,^{6,7} found that for β -Sn, $|\psi(0)|^2$ decreased when the tin sample was compressed. For β -Sn, $\gamma > 0$. The same qualitative result, $\gamma(\text{Sn}) > 0$, was also found for a number of tin alloys and compounds.⁷ An exception to this behavior was found for the intermetallic compound Mg_2Sn . For Mg_2Sn at low pressures, $\gamma(\text{Sn}) < 0$ was observed.

Möller and Mössbauer attributed the behavior of $|\psi(0)|^2$ with compression for β -Sn and for Sn alloys and compounds to a screening effect between the s and p valence electrons.^{6,7}

It would seem reasonable to inquire about the systematics of $\gamma(Z)$ with atomic number Z , i.e., to ask in what regions of the Periodic Table one might expect to find $\gamma(Z) > 0$. We have used the Wigner-Seitz-Dirac-Hartree (WS) model with Kohn-Sham or with Slater exchange to make a preliminary study of this question.^{8,9,10} Calculations were first made for the elements Ag-Te of the Periodic Table,⁸ and more recently they have been extended⁹ to the elements $1 \leq Z \leq 95$. These WS calculations were self-consistent including the core electrons.¹⁰ The compression of an atom was simulated by a decrease of the size of the WS sphere.^{3,8,9,10}

The WS model does not include the scattering of the electrons on the reciprocal lattice, and thus

it may not be expected to give a precise value for $\gamma(Z)$ for a particular element whether pure, in an alloy, or in a compound. For example, this model cannot account both for $\gamma(\beta\text{-Sn}) > 0$, and $\gamma(\text{Sn}) < 0$ for Mg_2Sn . In that the model is self-consistent,¹⁰ however, it may give an indication of the trend of $\gamma(Z)$ as Z increases and as the s , p , d , and f shells are filled. The WS model implies much variety and regularity in the behavior^{8,9} of $\gamma(Z)$ with Z . It may then be of value to study this indicated systematic behavior of $\gamma(Z)$ experimentally and to extend these calculations to include band-structure effects.

In agreement with Möller and Mössbauer, the WS model gives the result that $\gamma > 0$ for β -Sn is predominantly due to a screening effect between the valence s and p electrons.⁸ The WS model indicates in addition that the core contribution to γ is not negligible.⁸

In the Ag row of the Periodic Table, the elements Sn, Sb, Te, I, Xe, and then in the next row Cs, are suitable for the measurement of γ by use of the Mössbauer effect. This is a region of Z where the WS model implies $\gamma > 0$. The purpose of the present high-pressure studies is the measurement of γ for metallic Sb (Ref. 11) and for I^- , and to use these measurements in a first comparison with our preliminary study of $\gamma(Z)$ in the WS model.^{8,9}

II. THE HIGH-PRESSURE-LOW-TEMPERATURE MÖSSBAUER MEASUREMENTS

The Bridgman anvil clamp used to produce the high pressures in these Mössbauer measurements is illustrated in Fig. 1. Some details about the use of the clamp are given in the figure caption.

The isomer-shift-high-pressure data given below are plotted as a function of the average pressure P applied to the sample. This gives an acceptable treatment of the data if the change of the isomer shift ΔS between $P = 0$ and the highest P is small relative to the Mössbauer linewidth.³ This

is the case for the experiments reported here. The P values given below were calculated from the measured applied force at 300 K and the anvil area, and include¹¹ a contribution of a few percent due to cooling the clamp from 300 to 77 K. We estimate the error in P to be about $\pm 5\%$ at $P = 65$ kbars.

The Mössbauer radiation source was $\text{Ca}^{121m}\text{SnO}_3$, $E_\gamma = 37.15$ keV for the antimony measurements, and was $\text{Zn}^{127m}\text{Te}$, $E_\gamma = 57.60$ keV for the iodine measurements. The counting geometry was similar to that of an apparatus used previously.³ A two-atmosphere Xe proportional counter was used to count the ^{121}Sb escape peak. The ^{127m}Te radiation was counted with an $\text{NaI}(\text{Tl})$ scintillation counter. For the Sb measurements, the source and

absorber were at 77 K and for the I measurements, they were at 4.2 K. The Mössbauer transducer armature extended³ from the cold region to room temperature (296 K). A ^{57}Fe Mössbauer source was mounted on the armature at the 296-K end and a six-line Mössbauer spectrum of metallic Fe at 296 K was measured simultaneously with each Sb or I spectrum. This provided a simultaneous velocity calibration of the transducer for each Sb or I measurement.^{3,11}

Antimony foil samples of 13- to 25- μm thickness were prepared from 99.999% Sb either by vacuum evaporation or by compression in a pellet press.¹¹ KI (and also NaI) samples of about 60- μm thickness were also prepared in the pellet press.

III. INTERPRETATION OF MÖSSBAUER LINE-SHAPE DATA

As an example of the Mössbauer measurements, Fig. 2 shows a typical measured Sb line shape. This curve was measured at zero pressure. The curve through the measured points represents a least-squares fit of the theoretical line-shape function^{12,13} given by

$$N(v_s) = N(\infty) \left[(1 - C f_s) + C f_s \left(\frac{2}{\pi \Gamma_0} \right) \int_{-\infty}^{\infty} dv \frac{\exp(-T_A \{1 - 2\xi [(v - S)/\frac{1}{2}\Gamma_0]\}) / \{[(v - S)/\frac{1}{2}\Gamma_0]^2 + 1\}}{[(v - v_s)/\frac{1}{2}\Gamma_0]^2 + 1} \right]. \quad (1)$$

Equation (1) describes a single-line Lorentzian source moving with Doppler velocity v_s relative to a single-line absorber with effective thickness $T_A = f_A t_0 \sigma_0 (1 + \alpha)^{-1}$, where f_A is the absorber recoilless fraction, σ_0 in cm^2/mg is the maximum resonance absorption cross section, t_0 is the sample thickness in mg/cm^2 of the resonant isotope, and α is the internal-conversion coefficient. $N(v_s)$ is the integrated transmitted intensity at v_s , C is the fraction of $N(\infty)$ due to the Mössbauer γ rays, f_s is the source recoilless fraction, S is the absorber-isomer shift relative to $v_s = 0$, and Γ_0 is the natural linewidth for the nuclear transition. ξ determines the amplitude of the dispersion term, due to interference, in the coherent part of the absorption cross section.¹³

The integral in Eq. (1) is evaluated by closed form integration of the first two terms of the integrand obtained from a series expansion of the absorption exponential. The remainder of the integrand is numerically integrated using Gauss-Legendre quadrature. The shape of a spectrum is completely characterized by knowledge of Γ_0 , T_A , S , and ξ . The fitted parameters $C f_s$ (treated as one parameter) and $N(\infty)$ serve as velocity-independent scaling factors on the basic line shape. The fitting procedure used here constrains ξ and Γ_0 and allows T_A and S to be obtained by the least-squares minimization.

We note that the curve of Fig. 2 appears symmetric. In fitting Eq. (1) to our line-shape data for both Sb¹¹ and I⁻, no evidence for the dispersion term was found. Thus, we have used $\xi = 0$ in Eq. (1) in obtaining the isomer-shift results reported below for antimony and iodine. In fitting Eq. (1) to the Sb data, a natural linewidth $\Gamma_0 = \hbar/\tau = 1.052$ mm/sec was used.^{11,14} For ^{127}I we used $\Gamma_0 = 1.25$ mm/sec.

IV. MEASURED PRESSURE DEPENDENCE OF THE ISOMER SHIFT FOR METALLIC Sb AND I IN KI

A. Antimony

Figure 3 is a plot of the measured pressure dependence of the isomer shift for Sb¹¹. We have fitted these data with a straight line by a weighted least-squares method. We obtain

$$S(P) = S_0 + P \frac{dS}{dP}, \quad (2)$$

with

$$S_0 = -11.64 \pm 0.01 \quad (3)$$

in units of mm/sec and

$$dS/dP = +0.0030 \pm 0.0003 \quad (4)$$

in mm/sec kbar.

We have calculated, in the Debye model,¹¹ a

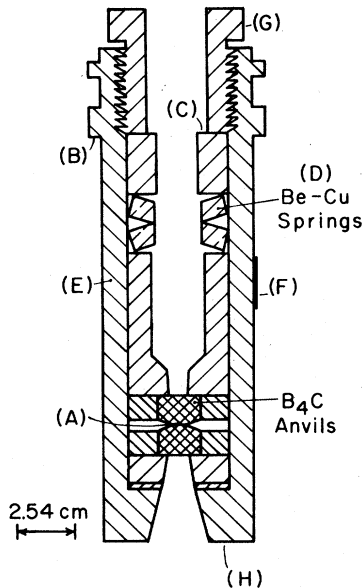


FIG. 1. The high-pressure clamp. In the following we give some details about the clamp and its use. The clamp was fabricated from the steel, Vascomax 300. The sample foil (Sb, NaI, or KI here) is clamped between the B_4C anvils at A. To clamp the foil, the cell is supported on the shoulder at B, and a measured force is applied at C with a hydraulic jack. The hydraulic pressure is measured with a calibrated Heise-Bourdon gauge. A strain gauge, cemented to the cell at F, was calibrated in terms of the force applied at C. When the desired force at C was attained, the nut G was gradually tightened while, at the same time, the force at C was removed. This was done at nearly constant strain gauge reading. The final force on the anvils, when the force at C was completely removed, was obtained from the strain gauge reading to about one percent. The length l of the cell between B and H was measured before and after every high-pressure measurement both with the sample at high pressure and at zero pressure. A vernier, reading to $2.5 \mu\text{m}$, was used to measure l . The length change Δl in μm was calibrated in terms of the force at C and was linear such that $\Delta l = 1.6 P \mu\text{m}$, where P is the average pressure on the sample in kbars (see text). After many cycles to high pressure, there was no change of the vernier reading, either for the sample at zero pressure, or between the beginning and end of a given measurement at high pressure. To the precision of the vernier (about 3% in P at $P = 65$ kbars) there was no permanent deformation of the cell, nor was there ever a loss of pressure on the sample during any experiment for many measurements. After many measurements to ~ 100 kbars, no plastic deformation of the B_4C anvil faces has been observed. In the present work on Sb, these circular faces have an area of $0.246 \pm 0.010 \text{ cm}^2$, and the Mössbauer gamma rays were collimated to pass through this area. When the clamp is cooled from 300 to 77 K the force on the sample increases by a few percent due both to contraction and to the increase of Young's modulus of the clamp components. The pressures reported include calculated values for this increase.¹¹

correction to dS/dP of Eqs. (2) and (4) due to the second-order Doppler shift.^{4,12} We obtained $-0.00004 \text{ mm/sec kbar}$. This is small compared with our error of measurement of dS/dP and has been omitted from the result, Eq. (4).

The intercept at zero pressure, S_0 , is slightly below the value measured by Ruby *et al.*¹⁵ They reported $-11.69 \pm 0.02 \text{ mm/sec}$.

The pressure dependence of the isomer shift^{3,11,12} may be described by

$$dS/dP = \frac{2\pi}{3} Z e^2 \delta \langle r^2 \rangle \frac{d|\psi(0)|^2/dP}{|\psi(0)|^2}. \quad (5)$$

$Z = 51$ is the atomic number of Sb, e is the electron charge, $\delta \langle r^2 \rangle = (-24.6 \pm 5) \times 10^{-29} \text{ cm}^2$ is the change of the average squared nuclear size¹⁷ between the excited and ground nuclear states, and $|\psi(0)|^2$ is the total electron probability density at the nucleus.

For ^{121}Sb , $\delta \langle r^2 \rangle < 0$. Thus our measured $dS/dP > 0$ corresponds to $d|\psi(0)|^2/dP < 0$. $|\psi(0)|^2$ decreases¹¹ when pressure is applied to metallic Sb.

Between 0 and 70 kbars, the average compressibility¹⁸ of Sb is $V^{-1}dV/dP = -17.9 \times 10^{-4} \text{ kbar}^{-1}$. Then from the above we obtain

$$\gamma = d|\psi(0)|^2/d \ln V = +8 \pm 3 \quad (6)$$

in atomic units. The large error is predominantly due to the uncertainty in $\delta \langle r^2 \rangle$.¹⁷

As we have noted, $\gamma > 0$ was first observed for Sn.^{5,6,7} Sb is the second element for which a decrease of $|\psi(0)|^2$ with increasing pressure has been observed.¹¹

B. Iodine

Figure 4 is a plot of the measured isomer shift, S for I^- in KI as a function of pressure. At $P = 0$, we obtain $S_0 = 0.164 \pm 0.014 \text{ mm/sec}$ relative to the ZnTe source. $S(P)$ is a straight horizontal line within experimental error, and gives no evidence of the phase transition circa 17.75 kbars.¹⁹ We find a slope $dS/dP = 0.00014 \pm 0.0007 \text{ mm/sec kbar}$ for an applied P up to 35 kbars. Thus we find $\gamma = 0$ within experimental error. We have made similar measurements with a NaI absorber, and find $\gamma(\text{NaI}) \approx 0$ also.

V. COMPARISON OF THE MEASURED $d|\psi(0)|^2/d \ln V$ WITH A CALCULATION IN THE WIGNER MODEL FOR Sn, Sb, AND I⁻

When a sample of metallic Sn or Sb, or of NaI or KI, is compressed, the average of the electron probability density over the unit cell will of course increase. In the immediate vicinity of the Sn, Sb, or I nuclei, however, the trend of the density, $|\psi(0)|^2$, with compression of the sample is differ-

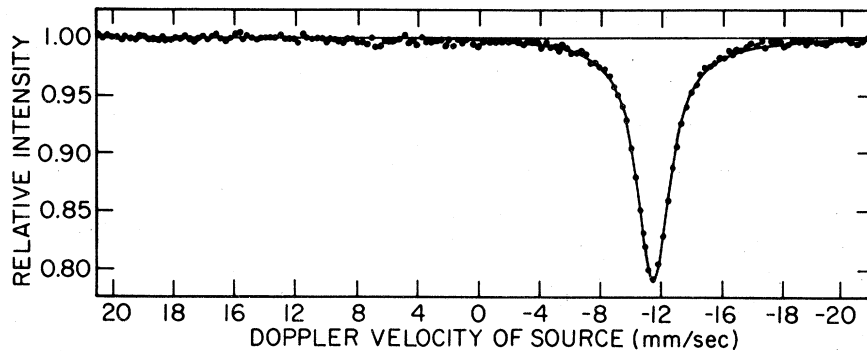


FIG. 2. An example of a Mössbauer spectrum for Sb taken at zero pressure. The Sb source has a low specific activity, and the counting rate was low. This curve represents three weeks of spectrometer time.

ent from this. The density, $|\psi(0)|^2$, decreases or remains constant with increasing pressure. For Sn or Sb, this corresponds to a movement of electron probability density outward from these nuclei into the interatomic region when the metal of normal density is compressed.

Figure 5 gives a plot of $\gamma(Z)$ for the elements

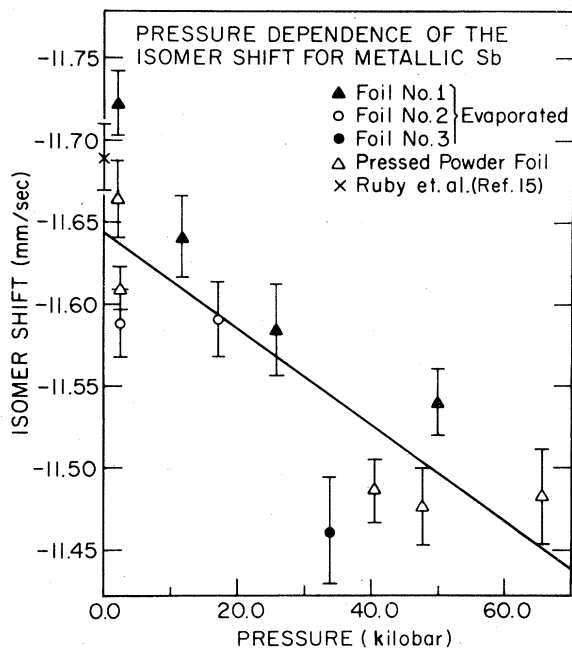


FIG. 3. Pressure dependence of the isomer shift for metallic Sb. The isomer shift becomes more positive with increasing pressure. Since $\delta \langle r^{-2} \rangle < 0$, this gives $d|\psi(0)|^2/dP < 0$. The charge density at the Sb nucleus decreases with increasing pressure. From measurements (Ref. 16) of the Sb Mössbauer linewidth for Sb metal and for the dilute alloy Cu(Sb), we find that any Sb nuclear quadrupole splitting of the Sb metal line is small compared with the linewidth, $\approx 0.01 (2\Gamma_0)$, and will not contribute to our measured value of dS/dP outside of the error given, Eq. (4).

Ag–Ba calculated in the WS model.^{8,9} For these elements, the WS model implies a narrow region of atomic number, ΔZ , for which $\gamma(Z) > 0$. This region is 3–5 elements wide and is centered at Te.

Figure 5 also shows measurements of $\gamma(Z)$ for β -Sn,^{5,6,7,8} Sb¹¹, and I⁻. $\gamma(\text{Sn})$ is above but $\gamma(\text{Sb})$ and $\gamma(\text{I}^-)$ are below the WS curve. For β -Sn and for Sn alloys and compounds, as we have recalled above, there is a spread of $\gamma(\text{Sn})$ values.^{5,6,7} A spread of $\gamma(\text{Sb})$ and $\gamma(\text{I}^-)$ must also occur for alloys or compounds of Sb and I. Thus, the experimental results plotted in Fig. 5 can, at best, only indicate a trend. The line connecting the experimental points is intended only to indicate a trend. With

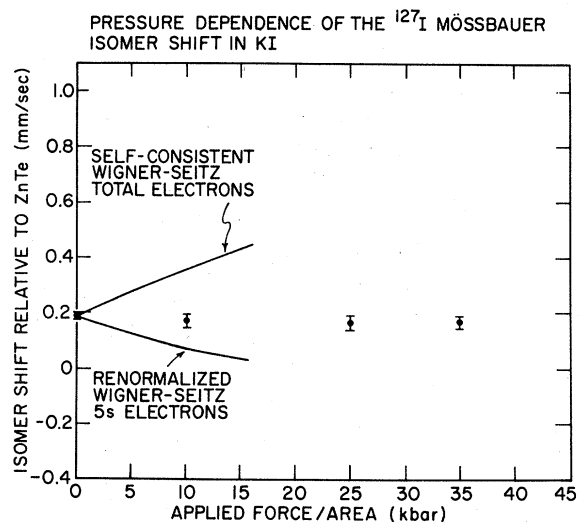


FIG. 4. Pressure dependence of the isomer shift for I⁻ in KI. The upper curve gives a calculation of this for I⁻ in the Wigner-Seitz model and the lower curve gives an estimate based on a simple renormalization of the zero-pressure, I⁻ ion, valence, WS wave function. Experiment falls in between with $dS/dP = 0.00014 \pm 0.0007$ mm/sec.kbar.

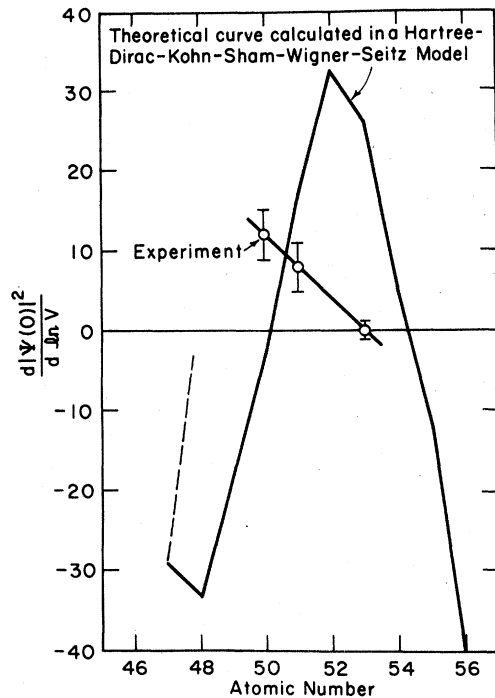


FIG. 5. A comparison is given here between an estimate of $\gamma(Z) = (d|\psi(0)|^2/d \ln V)_Z$ in the WS model^{8,9} and measurements of this quantity for Sn, Sb, and I⁻. The calculation implies a narrow region around Te of width $\Delta Z \sim 3-5$ for which $\gamma(Z) > 0$. With decreasing Z from I to Sn, experiment suggests an increasing $\gamma(Z)$. In the text we suggest that as Z decreases further below 50 (Sn), $\gamma(Z)$ will again be negative at least at Ag. This suggestion is indicated by the dotted line. $\gamma(\text{Ag})$ has not been measured. In the WS model $\gamma(\text{I}^0)$ and $\gamma(\text{I}^-)$ have nearly the same value. The WS value for $\gamma(\text{I}^0)$ is plotted here. The electron configurations used in these WS calculations of $\gamma(Z)$ for Ag–Ba were a core of filled inner shells through $(4d^{10})$ plus $5s_{1/2}$, $5s_{3/2}^2$, $5s_{3/2}^2 5p_{1/2}$, $5s_{3/2}^2 5p_{1/2}^2$, $5s_{3/2}^2 5p_{1/2}^2 5p_{3/2}$, $5s_{3/2}^2 5p_{1/2}^2 5p_{3/2}^2$, $5s_{3/2}^2 5p_{1/2}^2 5p_{3/2}^2 5p_{3/2}^2$, $5s_{3/2}^2 5p_{1/2}^2 5p_{3/2}^2 5p_{3/2}^2 6s_{1/2}$, and $6s_{3/2}^2$. Kohn-Sham exchange was used in these calculations.

decreasing Z from I to Sn, the trend of γ appears to be toward more positive values.

One may then inquire at which Z below 50 (Sn) one may again find by experiment $\gamma < 0$. The next element below Sn for which γ has been measured is Fe, $Z=26$. Here, indeed $\gamma < 0$ in qualitative agreement with the WS model.⁹ The nearest Mössbauer element below Sn where a Mössbauer experiment may be readily done is Ru at $Z=44$. The WS model⁹ gives $\gamma(44) < 0$.

For Au, both the WS model and experiment give $\gamma < 0$.^{3,10} Because of the many similarities of Au and Ag, it seems reasonable to suggest that with decreasing Z below Sn, one will again find $\gamma < 0$ at least at $Z=47$ for Ag or its compounds, as the WS model predicts. In Fig. 5, the dotted line rising from $Z=47$ is intended to suggest this. If this should prove to be the case experimentally, then the peak of $\gamma(Z)$ near Sn would have a width ΔZ of 3–5 but with the center of this region of Z having $\gamma(Z) > 0$ displaced several elements below the center of this region as implied by the WS model. $\gamma(\text{Ag})$ remains to be measured.

Thus far, for the elements Ag through Cs, only $\gamma(50)$ for β -Sn has been calculated in a band-structure model.²⁰ This calculation gave $\gamma(50) \approx -0.0$, a result which is roughly in accord with our Wigner-Seitz result,^{8,9} but not with experiment, Fig. 5.

We have shown that in the Wigner-Seitz model⁸ for Sn, even the sign of $\gamma(Z)$ is dependent on the treatment of exchange. A further experimental and theoretical study of the systematics of $\gamma(Z)$ may contribute to the understanding of electron-electron interaction effects as viewed from the innermost, high-electron-density, region of an atom.

ACKNOWLEDGMENT

This work was supported by the NSF under Grant No. DMR 7818916 to the University of North Carolina.

*This paper is based in part on the Ph.D. thesis of William T. Krakow.

†Present address: Bell Laboratories, Allentown, Pa. 18103.

‡Present address: Department of Physics, Colorado School of Mines, Golden, Colo., 80401.

¹R. V. Pound, G. B. Benedek, and R. Drever, Phys. Rev. Lett. **7**, 405 (1961).

²G. Kaindl, D. Salomon, and G. Wortmann, in *Mössbauer Effect Methodology*, edited by I. J. Gruverman (Plenum, New York, 1974).

³Louis D. Roberts, D. O. Patterson, J. O. Thomson,

and R. P. Levey, Phys. Rev. **179**, 656 (1969).

⁴D. L. Williamson, in *Mössbauer Isomer Shifts*, edited by G. K. Shenoy and F. E. Wagner (North-Holland, Amsterdam, 1978).

⁵V. N. Panyushkin and F. F. Voronov, Zh. Eksp. Teor. Fiz. Pis'ma Red. **2**, 97 (1965) [JETP Lett. **2**, 97 (1965)]; V. N. Panyushkin, Fiz. Tverd. Tela (Leningrad) **10**, 1915 (1968) [Sov. Phys.—Solid State **10**, 1515 (1968)].

⁶H. S. Möller and R. L. Mössbauer, Phys. Lett. **24A**, 416 (1967).

⁷H. S. Möller, Z. Phys. **212**, 107 (1968).

- ⁸D. L. Williamson, John H. Dale, W. D. Josephson, and Louis D. Roberts, *Phys. Rev. B* 17, 1015 (1978).
- ⁹Louis D. Roberts, C. Page, J. H. Dale, and W. D. Josephson, *Bull. Am. Phys. Soc.* 24, 427 (1979).
- ¹⁰T. C. Tucker, Louis D. Roberts, C. W. Nester, Jr., T. A. Carlson, and F. B. Malik, *Phys. Rev.* 178, 998 (1969).
- ¹¹William T. Krakow, Ph.D. thesis, University of North Carolina, Chapel Hill, 1978 (unpublished).
- ¹²H. Frauenfelder, *The Mössbauer Effect* (Benjamin, New York, 1962).
- ¹³D. J. Erickson, J. F. Prince, and Louis D. Roberts, *Phys. Rev. C* 8, 1916 (1973).
- ¹⁴*The Mössbauer Effect Data Index*, edited by J. G. Stevens and V. E. Stevens, (IFI/Plenum, New York, 1975).
- ¹⁵S. L. Ruby, H. Montgomery, and C. W. Kimball, *Phys. Rev. B* 1, 2948 (1970).
- ¹⁶P. A. Magill, C. T. Page, W. T. Krakow, P. A. Deane, W. D. Josephson, and Louis D. Roberts, *Bull. Am. Phys. Soc.* 25, 121 (1980).
- ¹⁷L. H. Bowen, in *Mössbauer Effect Data Index*, edited by J. G. Stevens and V. E. Stevens (IFI/Plenum, New York, 1972); G. M. Kalvius and G. K. Shenoy, *At. Data Nuc. Data Tables*, 14, 639 (1974).
- ¹⁸*American Institute of Physics Handbook*, 3rd ed., (McGraw-Hill, New York, 1972).
- ¹⁹S. N. Vaidya and G. C. Kennedy, *J. Phys. Chem. Solids* 32, 951 (1971).
- ²⁰J. E. Inglesfield, *J. Phys. Chem. Solids* 31, 1443 (1970).